DOI: https://doi.org/10.53350/pjmhs22161937

ORIGINAL ARTICLE

Identification of ZINC inhibitors for HIV-1 Protease through Structure-Based Pharmacophore, Virtual Screening, ADMET and Molecular Dynamics Simulation

ANDREW RABONTSI MOTSILANYANE[1], ZIMBILI MKHIZE[2], SPHELELE SOSIBO[3]
[1]*Department of Organic Chemistry and pharmaceutics, Faculty of Natural and Agricultural Sciences, North West University, South Africa*
[2]*Head of Department, Organic and Pharmaceutic Chemistry, Faculty of Natural and Agricultural Sciences, North West University, South Africa*
[3]*Lecture Department of Organic and Pharmaceutic Chemistry, Faculty of Natural and Agricultural Sciences, North West University, South Africa*
Corresponding author: Andrew Rabontsi Motsilanyane, Email: rabontsikya@gmail.com, Cell: +27828922208

ABSTRACT

Treating HIV is made difficult by the evolution of antimicrobial resistant mutants of that occurs in the life cycle of this virus. This has led to the evolution of numerous inhibition mechanism that intends to challenges the replication of this virus. One such approach is the application of molecular modelling in drug discovery. In this study the application of computer aided drug design were employed in finding an inhibitor that can contribute in finding a suitable drug candidate. Firstly, the ZINC database was screened using the Lipinski's rule of five, and compounds having similar biological features were classified and grouped together into a compound library. Secondly, the co-crystallized structure of 1rv7 wild type of HIV-1 protease was used to construct a pharmacophore model that was used to screen further, the ZINC database Ligand stored in the compound library. Thestructure-basedpharmacophore was created by mimicking the three main active features of the co-crystallized structure from the Protein Data Bank, namely, 82 and 84, I50 and I150 residues.Thirdly, a total of twenty-six of the compounds that had less than 0,5 RMSD were identified and selected. Fourthly, based on the best docking ligands, ten of these compounds having high binding affinity were selected. These compounds are ZINC_001456687980 (-8.0), ZINC_001445792073 (-7.8) and ZINC_001461099137 (-7.4), successively. However, ZINC_001461099137 was eliminated based on unfavorable donor-donor interaction. The subsequent compound, ZINC_000015276352 was then placed on the top three leading compounds with a binding affinity of (-6.9). Fifthly, the ADMET property analysis was used on the top ten compounds, and the compounds that satisfied the analysis were, ZINC_001456687980, ZINC_000015276352, ZINC_001359888321 and ZINC_001460445290. The main properties that included the BBB permeation, the gastrointestinal absorption, pan assay interference structure (PAINS), were analyzed. ZINC_001456687980 had two violation (mw >350, XLOGP3>3.5),whiles ZINC_000015276352 had three violations (mw > 350, XLOGP3 > 3.5, rotatable > 7). Lastly, only two top compound underwent molecular dynamics simulations. Molecular dynamics simulation revealed the formation of numerous bond interactions between ZINC_001456687980 and ZINC_000015276352 together with the target protein.

INTRODUCTION

Human immunodeficiency virus type 1 (HIV-1) acts as a cause of acquired immunodeficiency syndrome (AIDS)(Jette et al., 2021). Since the beginning of this epidemic, the global public health has incurred serious economic threats, whichhas led to minimal supply of pharmaceutical care in low-income countries(Michael et al., 2021). UNAIDS in 2020 report that, an estimated 37.7 million people were living with HIV, whiles, there are 1, 5 million infections leading to at least 680 000 deaths that are related to HIV(UNAIDS, 2020). In the quest to finding the cure for this disease, there has been an advent of more than 40 antiretroviral drug that targets various places in the life cycle of this virus. HIV-1 viral particle consists of two copies of single stranded viral RNA and the viral enzymes namely, the Integrase, the protease and the reverse transcriptase(Shin et al., 2021), (Haaland et al., 2021). These components of viral particles and enzymes are enveloped by capsid core(Guedán et al., 2021).

In the first stages of viral intrusion into the host cell, the gp120 of the virus begins by attaching itself to the CD4 receptor of the host, on the T-cell membrane. The gp41 from the gp120 are then released into host's cell in order to bind with chemokine co-receptors that includes the CCR5, CCR4 and CXCR4. This process causes a fusion between the viral envelop and the co-receptors. The viral components will then be released inside the host's cell, this step is followed by other processes that leads to the maturation of a viral species that can repeat the cycle and infect another host cell(Andrianov et al., 2021).

More than 1000 amino acids makes up two subunits namely the p66 and p51, whereby the binding region is found mainly within the p66. The p66 consists of sub domains namely; fingers, thumb, palm, connection and the RNase-H as proposed by Huang et al(Huang et al., 1998),(Huang et al., 2014), (Zheng et al., 2005). This therefore makes up the active sites where binding can occur. The P66 subunit contains 560 amino acids whiles the p51 contains 440 amino acids. The functional mechanics of HIV-1 protease involves three main target structures, which are the HIV-1 reverse transcriptase, RNase- H and the integrase. HIV-1 reverse transcriptase and RNase- H are responsible for reverse transcription of the ssRNA into the dsDNA strands and consequently cleaves to the RNA strand from the RNA/DNA hybrid respectively. Whereas, on the other hand the HIV-1 integrase facilitate the integration of viral DNA into the hosts genome(Ippolito et al., 2021).

In 1996 Dr David Ho proposed the High active antiretroviral therapy (HAART), in the fight against HIV, this has yielded great success(Finzi et al., 1997), (Ortiz et al., 1999, Shafer and Vuitton, 1999). However, its success was short-lived by the evolution of cross-resistant strains of HIV severe side effects and in some cases; there were observations of poor patient compliance of pill administration(Murri et al., 2000). This therefore paves a way for the need to find new and effective anti-HIV drug that can have minimal side effects on patients and has the ability to improved pharmacokinetic properties.

Over the years there has evolved a number of inhibition approaches that intends to interrupt the life cycle of HIV-1 protease. This has been brought about by the contribution in the scientific fraternity, and one such contribution was made by Chen and his group who proposed that, the binding pocket of the HIV-1 protease undergoes some changes in the shape and conformation upon certain drug-resistant mutations. They further made an observation that as a results of this mutation there is a reduction in the binding affinity of the inhibitor, this lead to recent advancements about the flaps on the protein, and in studies made in understanding their morphology and physiological activities(Chen et al., 2005) .

The recent finding performed through coarse-gained molecular dynamics simulation observed a spontaneous opening and reclosing of the flaps. These studies were performed by Tozzini et al, who independently observed the fluctuation between semiopen, closed and fully open conformation at 30 ns and four different conformation between closed, semi-open, open and wide open, respectively. From the early studies of molecular dynamic

simulation, which suggested a closed ligand free conformation to the recent studies that observed the four conformation of the HIV-1 protease, demonstrate that, through the study of molecular dynamics and simulation, there is a gap that needs the be filled by understanding the mechanism of the protease(Trylska et al., 2007).

In this study,computer aided drug design was used to screen and filter compounds from the ZINC database in an attempt to find a suitable drug candidate using pre-existing drugs. This procedure has yielded great success in the past, with numerous ARVs being discovered using this approach (Leelananda and Lindert, 2016), (Zhao et al., 2020). The search for a drug with similar features and biological properties to the drugs that are in the market is one the most fundamental tools to be used in the current period of drug discovery (Hussain et al., 2021).

MATERIALS AND METHODS

Below is a flowchart prescribed for the computer aided drug design and its methodology.

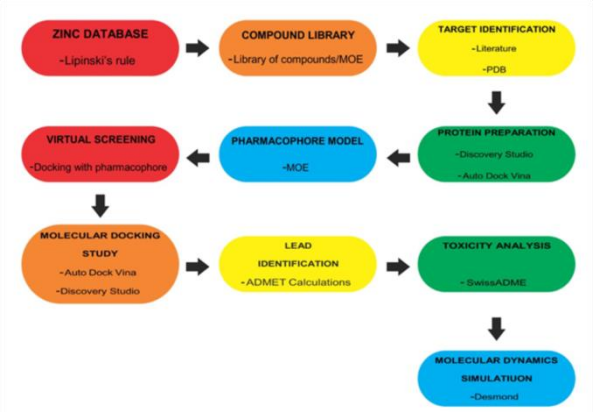

Figure 1: The Flowchart of adopted computer-aided drug design (CADD) methodology.

4.2.1 Zinc database

The compounds in the ZINC database were screened using the Lipinski's rule of five. A total of 497 891 compounds that were retrieved from the database. These compounds satisfied the application of the Lipinski's rule of five.

4.2.2 Compound Library

A library of these ZINC compounds was created on the MOE software. All these compounds will be screened with the pharmacophore.

4.2.3 Target Identification

Through literature, the protein was identified and retrieved from the PDB database. This protein has a code of 1rv7.

4.2.4 Protein preparation

Discovery Studio was used to prepare the downloaded protein, as it was stored in the PDB as a co-crystallized structure.(Adeniji et al., 2020)

4.2.5 Pharmacophore Model

A pharmacophore model was developed on the base of the co-crystal compound with protein by MOE. The query was saved. The features from the co-crystallized structure retrieved from the database were employed in constructing the pharmacophore model that will be used for virtual screening(Achiri et al., 2021).

4.2.6 Virtual Screening, Docking with pharmacophore

The prepared library of the compounds obtained through the rule of five was screened on the bases of a developed pharmacophore query(Tariq et al., 2021).

4.2.7 Molecular Docking study

The docking studies between the screened ZINC compounds was performed. In this analysis, a blind docking was executed with a grid box that was generated in X, Y and Z axis as follows: center_x = 19.1732 center_y = 41.6246 center_z = 0.0403 size_x = 37.819451558 size_y = 37.9149091911 size_z = 58.311979351. The binding affinity between the ligand and the protein was obtained after docking and their interaction was observed on discovery studio and PyMOL. The compounds that had the best hits from docking studies were analyzed. Their 2D and 3D interaction were evaluated using the discovery studio.

4.2.8 ADMET Calculation

Safety evaluation these ZINC compound was employed using the SwissADME web server. This evaluation involves the adsorption, distribution, metabolism, excretion and toxicity (ADMET) characteristic profiling(Daina et al., 2017).

4.2.9 Molecular Dynamics Simulation

The Desmond package, which is part of Schrödinger LLC, was used to perform molecular dynamics and simulation at 200nanoseconds(Gopinath and Kathiravan, 2021). This procedure is important was performed after molecular docking studies, which predicts the ligand binding position in its static condition. The docking predicts the characteristic binding nature of the ligands together with the protein in the physiological environment. After it was preprocessed, the ligand-protein complex was optimized and minimized using Maestro.

A 0.15 M salt (NaCl) was added in order to mimic the physiological environment which the simulation will take place in. In addition, the following variables were ensemble as moles (N), temperature (T) and pressure (P) and for a complete simulation. A 1 atm pressure and 300 K temperature were selected. The trajectory was saved at 100ps, with a simulation time of 200ns at the energy of 1,2. The pressure bar was at 1.01325 with following estimated 25 390 number of atoms. The root mean square deviation (RMSD), root mean square fluctuation (RMSF) were analyzed and the stability of the simulation was evaluated(Xu et al., 2012).

RESULTS

In Silico Analysis: Based virtual screening

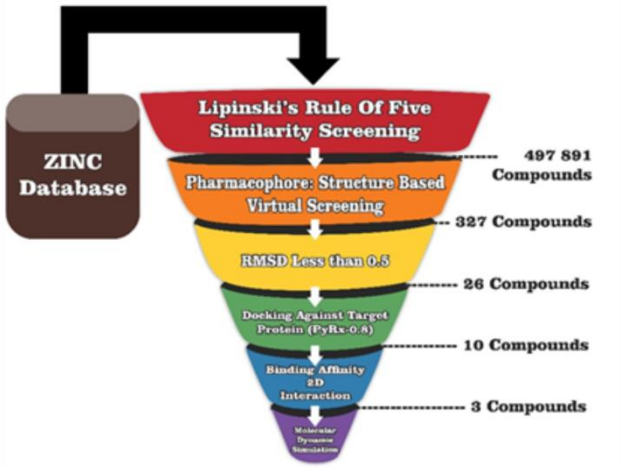

Figure 2:The flowchart highlighting the filtering of ZINC compounds

4.3.1 Druglikeness Analysis: A proposed lead compound was determined by following the flowchart through virtual screening processes, as shown by figure 1. This approach has been used in research, since it filters and incorporates various compounds that has common drug-likeness(Ouyang et al., 2021). Through these processes, it was possible to mimic the co-crystalized structure through structure based pharmacophoric screening and later analyze the ligand-protein complexes through molecular dynamics simulation. Drug analysis follows a computational approach that includes the Lipinski's rule of five, that predicts that absorption is more likely when the compounds displays, less than 5 hydrogen bonds, less than 10 hydrogen bonds, molecular weight (mw) is

less than 500 and the calculated LogP is less than 5(Lipinski et al., 1997). In the process, molecular docking wasapplied in order to analyze the interactions between the ligand and the target protein. Ligand-protein contacts, root mean square deviation and root mean square fluctuation are some of characteristics that were analyzed using molecular dynamics simulation, which computational approach that capture the behavior of protein and the ligand(Hollingsworth and Dror, 2018).

Figure 3: An uncomplexed HIV-1 protease

4.3.2 Virtual Screening of HIV-1 Protease Inhibitors Using ZINC Databank and AutoDock Vina Applying the Lipinski's Rule of Five: Molecules were retrieved from the ZINC database. These ligands were searched based on their likeness in chemical composition. For the effectiveness of this search, the Lipinski's rule of five was employed and a total of 497 891 ligands were found on the ZINC database.The compounds in the ZINC database are a collection commercially available compounds. These compounds are suitable for screening using the database.

4.3.3 Development of A pharmacophore model on the basis of the co-crystal compound with protein by molecular operating environment. (**Structure based pharmacophore modelling):** Pharmacophore technique based on the co-crystallized mimicry.

A pharmacophore model was built using a structure-based modelling approach. This model is based on obtaining compounds that are available for inhibitor binding of HIV 1 protease using its co-crystallized structure. Three active pharmacological features were identified namely, (F1: Don and Acc), (F2: Acc) and (F3: Don). This technique of creating the pharmacophore features is determined by the contacts and bonds found on the hot-spot residues. For this determination, a pharmacophore query editor tool of MOE 2014.09 software was used to facilitate this process(Kobayakawa et al., 2021).

These feature (F1: Don&Acc, F2: Acc and F3: Don) are the active parts of the 1vr7 receptor that has been mimicked as the original (F1: Don&Acc, F2: Acc and F3: Don) mimetic inhibitors that were used to design 1vr7 Co-crystal structure. A library for the 497 891 compounds was created on the MOE 2014.09 software and these compounds were docked with pharmacophore. Based on the pharmacophore-fit, a total of 327 compounds was retrieved.

Table 1: Interaction between the trio hot-spot residues of 1vr7 co-crystal structure and the corresponding residues of the 1vr7 receptor at the binding site (PDB ID: xxx)

1vr7 hot-spot residue	Type of interaction	Residue
F1 = Don/Acc	σ carbon-carbon bond	82 and 84
F2 = Acc	Van der Waals	I50
F3 = Don	Hydrogen bonds	I150

Through modeling studies, Logsdon et al discovered a strange behaviour of a mutant strain HIV-1 MDR 769 that was isolated clinically from a patient who was failing extensive antiretroviral therapy. This outcome was as a result of viremia, a medical condition in which the viruses was present in the bloodstream. The isolated strain of an HIV-1 MDR 769 protease was examined through expresssion, purification and crystallization and it was discovered that, there was an expassion on the active site of the protease. That expansion was the one responsible for the deacrese in the volume of amino acids leading to the loss of van der Waals, hydrogen bonds and σ carbon-carbon bond(Logsdon et al., 2004). Thus, causing a decrease in the protein-ligand binding affinity. The derived strain of 1rv7 complex was deposited in the Protein Data Bank for further scientific studies and it is the very same co-crystallized structure used in this project to create a pharmacophore model.

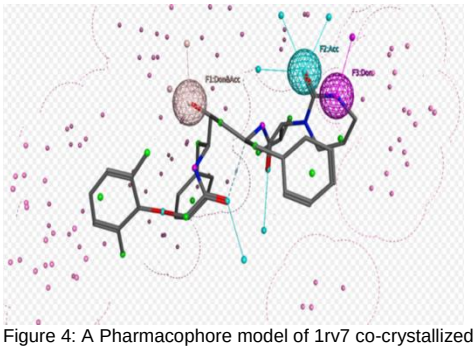

Figure 4: A Pharmacophore model of 1rv7 co-crystallized structure.

4.3.4 Ligand-Pharmacophore properties based on the RMSD: From the 327 ligands that were fitted with the pharmacophore, 26 compounds with the RMSD of less than 0,5 were selected.

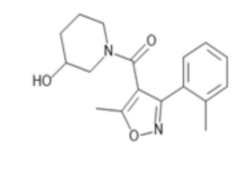

zinc_001456687980

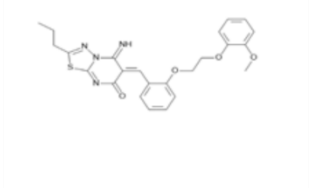

zinc_001461099137

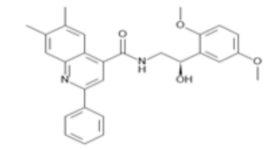

zinc_001445792073

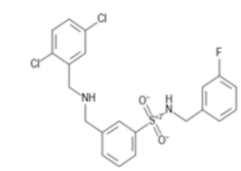

zinc_000015276352

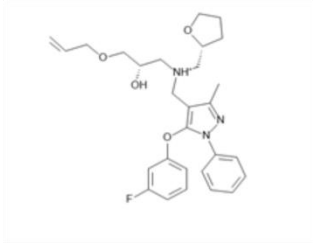

zinc_000036146610

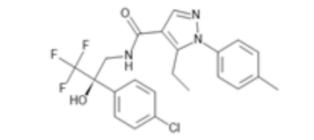

zinc_001445348172

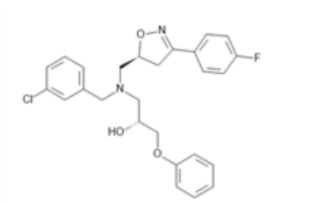

zinc_0000363464

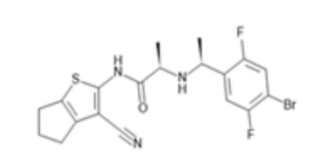

zinc_001359888321

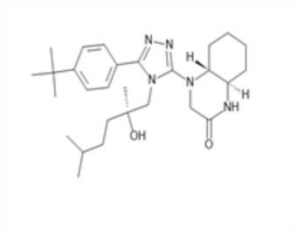

zinc_001460445290

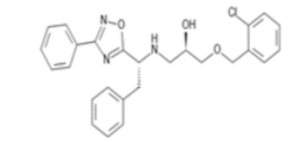

zinc_000003384470

4.3.5 Molecular docking against target protein: These 26 ligands were selected for molecular docking with the target protein. The features of the top 10 ligands are shown below was performed through Autodock Vina.

5.3.6 SwissADME studies: SwissADME/T web server was employed to predict the absorption, distribution, metabolism, excression and toxicity of zinc_001456687980 and zinc_000015276352. Table 3 shows the predicted value for both compounds, for iLOGP, XLOGP, MLOGP, WLOGP and SILICOS-IT models.

Table 3: SwissADME properties analysis

Zinc ID	M.W	Binding Affinity	iLOGP	XLOGP3	WLOGP	MLOGP	SILICOS-IT	C/SUS LOG P O/W
*1.zinc_001456687980	455.34	-8	3.36	4.10	4.36	3.36	5.13	4.06
2.zinc_001445792073	456.53	-7.8	4.04	4.65	4.67	2.77	5.84	4.39
3.zinc_001461099137	453.36	-7.4	3.89	4.60	5.30	4.40	5.16	4.67
*4.zinc_000015276352	464.54	-6.9	3.93	4.69	3.22	2.13	5.82	3.96
5.zinc_001445348172	451.87	-6.9	3.97	4.77	5.73	3.63	4.95	4.61
6.zinc_000036146610	468.95	-6.8	4.05	5.16	4.80	3.80	5.94	4.75
7.zinc_000036346408	496.56	-6.8	4.76	4.38	3.51	-0.59	4.91	3.39
8.zinc_001359888321	481.67	-6.7	4.25	5.22	3.92	3.50	4.19	4.21
9.zinc_001460445290	454.33	-6.7	3.33	4.86	5.15	3.43	6.34	4.62
10.zinc_000003384470	463.96	-6.6	3.80	4.55	4.36	2.91	5.51	4.23

From the 10 compounds with the best binding affinity, only two passed the Swiss ADME test (Highlighted with green). Four compounds namely zinc_001456687980, zinc_000015276352, zinc_001359888321 and zinc_001460445290, were predicted to be suitable for oral administration.

Table 4: SwissADMET properties Ligand ID QPlogPo/v QPLogHERGQPPCacoQPlogBB QlogKhsa

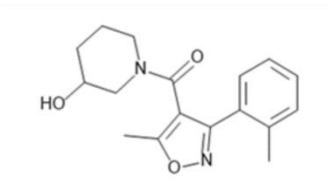

A. Zinc_001456687980 4.797-5.553 1802.65-0.12 0.818

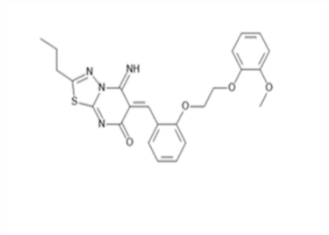

B. Zinc_000015276352 4.901 -6.858 872.832 -1.269 0.544

Table 5: SwissADME/T properties for Lead Compounds

Properties of lead compounds	Zinc_001456687980	Zinc_000015276352
Molecular weight	455.34	464.54
Toxicity	Non-toxic	Non-toxic
Ring	3	4
Carcinogenetic	Non-carcinogenic	Non-carcinogenic
Solubility	Moderately Soluble	Moderately Soluble
Binding Energy	-8	-6.9
Molar refractivity	119.22	130.60
H-bond Acceptor	4	7
H- bond Donor	1	1
GI absorption	High	High
BBB permeation	Yes	No
Leadlikeness	MW > 350; XLOGP3 > 3, 5	MW > 350; XLOGP3 > 3, 5, Rt >7
Abbott BA	0.55	0.55
Skin Permeation	-6.17 cm/s	- 5.80 cm/s
PAINS	0.Alert	0.Alert

In Swiss ADME/T web server was used to determine various toxicity parameters, metabolizing enzyme interaction and absorption parameters. This was done on the basis of the screened structures and molecules that were obtained for drug-likeness character. Table 5 gives a brief overview of some of the important parameters based on the following criterion: The criterion were based on the following parameters: Mol. W 130 – 725: donorHB 0-6: accptHB 02 –20: QPlogPo/w (-2-6.5) below - : QPlogHERG 5: QPPCaco < 25 => poor >500 => great: QPlogBB (-3 – 1.2): QPlogKhsa (-1.5 – 1.5)

4.3.6 Binding Affinity: 2D interaction

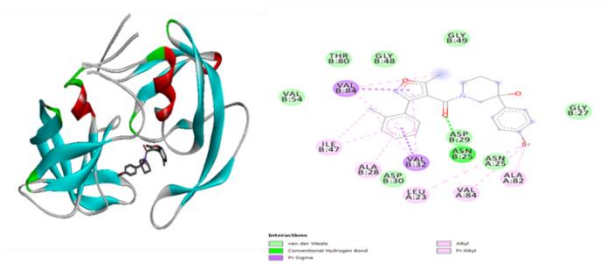

A. Zinc_001456687980

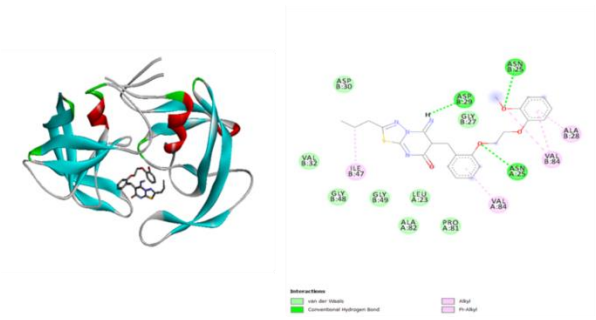

B. Zinc_000015276352

Figure 5: Binding interaction of ZINC compounds and 1rv7.

Table 6: The docked Van der Waals, Conventional Hydrogen Bonds, Pi-Sigma, Alkyl, Pi-Alkyl between 1rv7 protein and best 3 compounds

Compounds	Van der Waals	Conventional H bonds	pi-sigma	Alkyl	pi-alkyl	
1. Z_001456687980	Gly49, Gly48, Thr80,	Asn25.	Val32, Val84.	Ile47, Ala28.	Val54, Asp30, Asp29	Asn25, Gly27
2. Z_000015276352	Asp30, Val32, Gly48	Asn25, Asp29.	Val84, Ala28	Ale47	Gly49, Ala82, Leu23,	Pro81, Gly27.

Figure 5 shows the orientation and interaction of Zinc_001456687980 and

Zinc_000015276352 at 1rv7 active site. Both Zinc_001456687980 and

Zinc_000015276352 shows binding in the active side and are located inside the binding pocket of the protein. Zinc_001456687980 displays the following the following hydrogen bod interactions Gly49, Gly48, Thr80, Val54, Asp30, Asp29, Asn25, Gly27. Hydrogen bonds are very important in binding of drug to the receptor, and their formation shows a certain potential that the complex can possess. As revealed by the interaction, the hydrogen bonds occurred between two strongly negative charged groups, and this, increases the strength and the stability of the drug-receptor significantly. These Hydrogen bonds were formed by CH_2 of cyclohexane with Asn25 residue. They also participated with conventional hydrogen bonding interaction with the ligand. Other participations included the alky interactions with Ile47, Ala28 and pi –alky interactions with Leu23, Val84, Ala82. Moreover, 1rv7 has a hydrophobic active site. In this active site, the ligand is scaffolder and positioned. In the case ofZinc_000015276352 , three hydrogen bonds were formed namely, Asn_B25, Asn_A25 and Asp29. Based on the key residues and the interaction analysis between ligands and protein proposed, Zinc_ 001456687980 and Zinc_000015276352 possess properties

4.4 Molecular Dynamics Simulation: Using molecular dynamics simulation the following Desmond simulation trajectories were analyzed; the root mean square fluctuation, the root mean square deviation and the protein-ligand contact calculation, were the protein-ligand contacts was calculated from the MD trajectory analysis

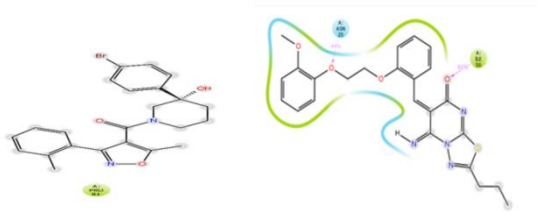

A. Z_001456687980 B. Z_001456687980

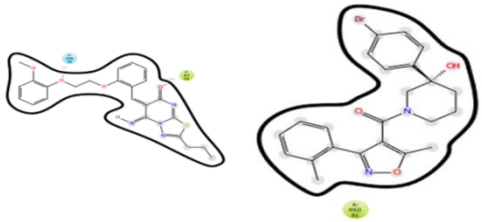

A. Z_000015276352 B. Z_000015276352

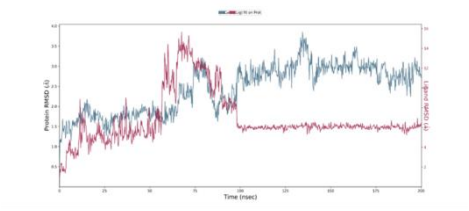

Figure 6: Ligand- Protein contacts

A.Z_001456687980

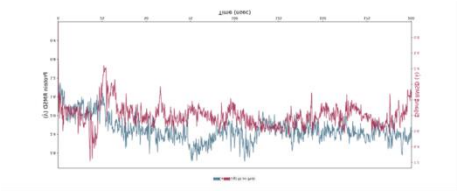

B. Z_000015276352

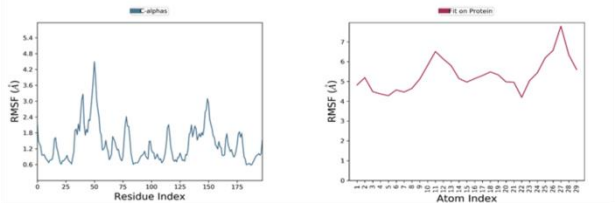

Figure 7: The diagrams A and B is obtained from Molecular dynamics Simulation and is of the root mean square deviation of the C-α atoms of the protein and the ligand with time in nano seconds (nsec). In this diagram the left γ- axis shows the variation of protein RMSD through time whereby, the right γ- axis shows the variation of the ligand RMSD through time.

Using the Desmond software, which is a package of the Schrödinger, the root mean square deviation (RMSD) trajectories were used to measure the scale of the distance between the ligand and the protein that takes place throughout the entire simulation. The interaction of the trajectories between the ligand and the protein were analyzed using the C-α atoms at time 200 nanoseconds. The structural conformation between the ligand and the protein were also determined throughout the simulation by monitoring the RMSD. This simulation reveals interactions when it reaches equilibrium and monitors the deviation that occurs in the thermal average. RMSD indicated that zinc_001456687980, at time 100ns reaches equilibrium until the end of the simulation 200ns. This complex remained at equilibrium with minimal fluctuations, and over the period of 100ns there was a decrease in the conformation for the receptor-ligand complexed. Towards the end of the simulation, zinc_001456687980 and zinc_000015276352,for ligand interaction shows values of 6 Å and 3.8 Å respectively, displaying zinc_000015276352 as a compounds having least value of Å.

Figure 8 shows images of the protein root mean square fluctuation (RMSF), which analyzes the C-α atoms with the peaks that shows the areas that fluctuates the most, which is indicated on the y-axis. Whereas the x-axis indicates, the residue location within that is found in the protein. The graphs for both compounds, shows major peaks at 50ns and 150ns for both compounds. Overlaying the RMSF yields (figure 10), which is a protein secondary structure. Secondary structures like beta and alpha helices are usually more rigid, meaning they are not flexible, as compared to the unstructured part of the protein. Therefore, these secondary structure fluctuates less.

Figure 6. Shows the ligand-protein contacts for zinc_001456687980and zinc_000015276352. The compounds that shows more than 30% interactions are shown. For zinc_000015276352, Asn25 and Ile50 display 44 % and 50%, respectively. And, for zinc_001456687980 Pro81, displays hydrophobic interaction for Pro81. This compound shows solvent exposure on all carbon bonds, nitrogen and oxygen atoms.

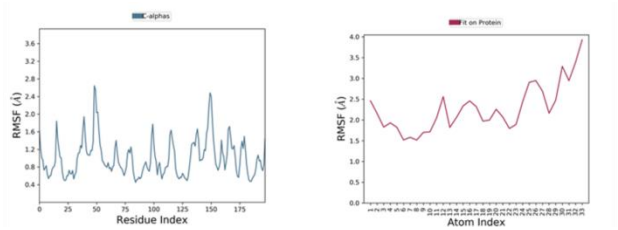

A.Z_001456687980/ P B. Z_001456687980/ L

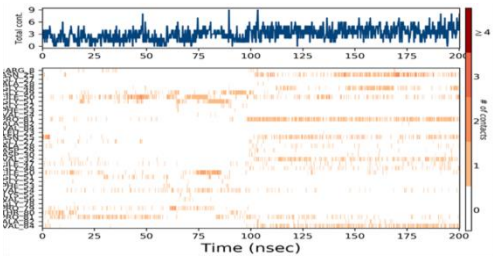

A. Z_000015276352/ P B. Z_000015276352/ L

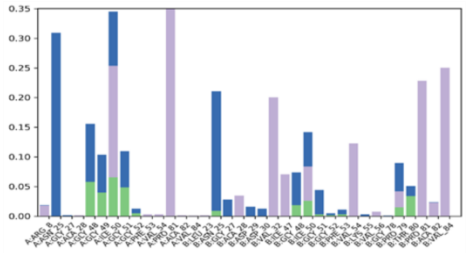

Figure 8: RMSFP/L for lead compounds

A. Z_001456687980
B. Z_000015276352

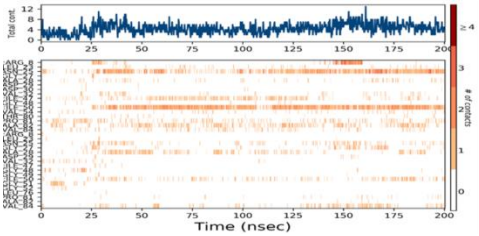

Figure 9: Protein-Ligand contacts

A. Z_001456687980
B. Z_000015276352

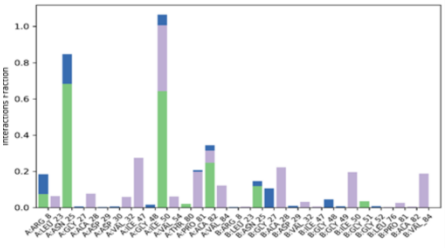

Figure 10: Protein-ligand contact histogram

Figure 9 shows the protein-ligands contacts for zinc_001456687980 and zinc_000015276352. zinc_000015276352 displays the following main interactions, Asn 25, Ile50, Ala82, whiles for zinc_001456687980 the intearctions are Pro81, Gle50 and Asn25. Figure 10, shows the bond length 0.7 for Asn25 and 0,6 for Ile50. Ile50 is also having 0,7 bond lenghth in compound zinc_001456687980.

REFRENCES

1. A PUBLICATION OF THE SOUTHERN AFRICAN HIV CLINICIANS SOCIETY. 2021. HIV NURSING MATTERS [Online]. Available: https://sahivsoc.org/Files/Nursing%20matters%20May%202017 [Accessed].
2. ACHIRI, R., FOUZIA, M., BENOMARI, F. Z., DJABOU, N., BOUFELDJA, T., MUSELLI, A. & DIB, M. E. A. 2021. Chemical composition/pharmacophore modelling-based, virtual screening, molecular docking and dynamic simulation studies for the discovery of novel superoxide dismutase (SODs) of bioactive molecules from aerial parts of Inula Montana as antioxydant's agents. Journal of Biomolecular Structure and Dynamics**,** 1-22.
3. ADENIJI, S. E., ARTHUR, D. E. & OLUWASEYE, A. 2020. Computational modeling of 4-Phenoxynicotinamide and 4-Phenoxypyrimidine-5-carboxamide derivatives as potent anti-diabetic agent against TGR5 receptor. Journal of King Saud University-Science, 32**,** 102-115.
4. ANDRIANOV, A. M., NIKOLAEV, G. I., SHULDOV, N. A., BOSKO, I. P., ANISCHENKO, A. I. & TUZIKOV, A. V. 2021. Application of deep learning and molecular modeling to identify small drug-like compounds as potential HIV-1 entry inhibitors. Journal of Biomolecular Structure and Dynamics**,** 1-19.
5. CHEN, B., VOGAN, E. M., GONG, H., SKEHEL, J. J., WILEY, D. C. & HARRISON, S. C. 2005. Structure of an unliganded simian immunodeficiency virus gp120 core. Nature, 433**,** 834-841.
6. DAINA, A., MICHIELIN, O. & ZOETE, V. 2017. SwissADME: a free web tool to evaluate pharmacokinetics, drug-likeness and medicinal chemistry friendliness of small molecules. Scientific reports, 7**,** 1-13.
7. FINZI, D., HERMANKOVA, M., PIERSON, T., CARRUTH, L. M., BUCK, C., CHAISSON, R. E., QUINN, T. C., CHADWICK, K., MARGOLICK, J. & BROOKMEYER, R. 1997. Identification of a reservoir for HIV-1 in patients on highly active antiretroviral therapy. Science, 278**,** 1295-1300.
8. GOPINATH, P. & KATHIRAVAN, M. 2021. Docking studies and molecular dynamics simulation of triazole benzene sulfonamide derivatives with human carbonic anhydrase IX inhibition activity. RSC Advances, 11**,** 38079-38093.
9. GUEDÁN, A., CAROE, E. R., BARR, G. C. & BISHOP, K. N. 2021. The Role of Capsid in HIV-1 Nuclear Entry. Viruses, 13**,** 1425.
10. HAALAND, R. E., MARTIN, A., MENGESHA, M., DINH, C., FOUNTAIN, J., LUPO, L. D., HALL, L., CONWAY-WASHINGTON, C. & KELLEY, C. F. 2021. Evaluation of Antiretroviral Drug Concentrations in Minimally Invasive Specimens for Potential Development of Point-of-Care Drug Assays. AIDS Research and Human Retroviruses.
11. HOLLINGSWORTH, S. A. & DROR, R. O. 2018. Molecular dynamics simulation for all. Neuron, 99**,** 1129-1143.
12. HUANG, H., CHOPRA, R., VERDINE, G. L. & HARRISON, S. C. 1998. Structure of a covalently trapped catalytic complex of HIV-1 reverse transcriptase: implications for drug resistance. Science, 282**,** 1669-1675.
13. HUANG, J., KANG, B. H., PANCERA, M., LEE, J. H., TONG, T., FENG, Y., IMAMICHI, H., GEORGIEV, I. S., CHUANG, G.-Y. & DRUZ, A. 2014. Broad and potent HIV-1 neutralization by a human antibody that binds the gp41–gp120 interface. Nature, 515**,** 138-142.
14. HUSSAIN, W., RASOOL, N. & KHAN, Y. D. 2021. Insights into Machine Learning-based approaches for Virtual Screening in Drug Discovery: Existing strategies and streamlining through FP-CADD. Current Drug Discovery Technologies, 18**,** 463-472.
15. IPPOLITO, J. A., NIU, H., BERTOLETTI, N., CARTER, Z. J., JIN, S., SPASOV, K. A., CISNEROS, J. A., VALHONDO, M., CUTRONA, K. J. & ANDERSON, K. S. 2021. Covalent Inhibition of Wild-Type HIV-1 Reverse Transcriptase Using a Fluorosulfate Warhead. ACS Medicinal Chemistry Letters, 12**,** 249-255.
16. JETTE, C. A., BARNES, C. O., KIRK, S. M., MELILLO, B., SMITH, A. B. & BJORKMAN, P. J. 2021. Cryo-EM structures of HIV-1 trimer bound to CD4-mimetics BNM-III-170 and M48U1 adopt a CD4-bound open conformation. Nature communications, 12**,** 1-10.
17. KOBAYAKAWA, T., YOKOYAMA, M., TSUJI, K., FUJINO, M., KURAKAMI, M., BOKU, S., NAKAYAMA, M., KANEKO, M., OHASHI, N. & KOTANI, O. 2021. Small-Molecule Anti-HIV-1 Agents Based on HIV-1 Capsid Proteins. Biomolecules, 11**,** 208.
18. LEELANANDA, S. P. & LINDERT, S. 2016. Computational methods in drug discovery. Beilstein journal of organic chemistry, 12**,** 2694-2718.
19. LIPINSKI, C. A., LOMBARDO, F., DOMINY, B. W. & FEENEY, P. J. 1997. Experimental and computational approaches to estimate solubility and permeability in drug discovery and development settings. Advanced drug delivery reviews, 23**,** 3-25.
20. LOGSDON, B. C., VICKREY, J. F., MARTIN, P., PROTEASA, G., KOEPKE, J. I., TERLECKY, S. R., WAWRZAK, Z., WINTERS, M. A., MERIGAN, T. C. & KOVARI, L. C. 2004. Crystal structures of a multidrug-resistant human immunodeficiency virus type 1 protease reveal an expanded active-site cavity. Journal of virology, 78**,** 3123-3132.
21. MICHAEL, H. U., NAIDOO, S., MENSAH, K. B., RAMLALL, S. & OOSTHUIZEN, F. 2021. The impact of antiretroviral therapy on neurocognitive outcomes among people living with HIV in low-and middle-income countries (LMICs): a systematic review. AIDS and Behavior, 25**,** 492-523.
22. MURRI, R., AMMASSARI, A., GALLICANO, K., DE LUCA, A., CINGOLANI, A., JACOBSON, D., WU, A. W. & ANTINORI, A. 2000. Patient-reported nonadherence to HAART is related to protease inhibitor levels. Journal of acquired immune deficiency syndromes (1999), 24**,** 123-128.
23. ORTIZ, G. M., NIXON, D. F., TRKOLA, A., BINLEY, J., JIN, X., BONHOEFFER, S., KUEBLER, P. J., DONAHOE, S. M., DEMOITIE, M.-A. & KAKIMOTO, W. M. 1999. HIV-1–specific immune responses in subjects who temporarily contain virus replication after discontinuation of highly active antiretroviral therapy. The Journal of clinical investigation, 104**,** R13-R18.
24. OUYANG, Y., HUANG, J.-J., WANG, Y.-L., ZHONG, H., SONG, B.-A. & HAO, G.-F. 2021. In Silico Resources of Drug-Likeness as a Mirror: What Are We Lacking in Pesticide-Likeness? Journal of Agricultural and Food Chemistry, 69**,** 10761-10773.
25. SHAFER, R. & VUITTON, D. 1999. Highly active antiretroviral therapy (HAART) for the treatment of infection with human immunodeficiency virus type 1. Biomedicine & pharmacotherapy, 53**,** 73-86.
26. SHIN, Y. H., PARK, C. M. & YOON, C.-H. 2021. An Overview of Human Immunodeficiency Virus-1 Antiretroviral Drugs: General Principles and Current Status. Infection & Chemotherapy, 53**,** 29.
27. TARIQ, A., REHMAN, H. M., MATEEN, R. M., ALI, M., MUTAHIR, Z., AFZAL, M. S., SAJJAD, M., GUL, R. & SALEEM, M. 2021. A CADD Based Discovery of Lead-Like Compounds Against KDM5A for Cancers Using Pharmacophore Modeling and High-Throughput Virtual Screening. Proteins: Structure, Function, and Bioinformatics.
28. TRYLSKA, J., TOZZINI, V., CHIA-EN, A. C. & MCCAMMON, J. A. 2007. HIV-1 protease substrate binding and product release pathways explored with coarse-grained molecular dynamics. Biophysical journal, 92**,** 4179-4187.
29. UNAIDS. 2020. HIV and AIDS in South Africa [Online]. Available: https://www.unaids.org/en/resources/fact-sheet. [Accessed].
30. XU, C., CHENG, F., CHEN, L., DU, Z., LI, W., LIU, G., LEE, P. W. & TANG, Y. 2012. In silico prediction of chemical Ames mutagenicity. Journal of chemical information and modeling, 52**,** 2840-2847.
31. ZHAO, L., CIALLELLA, H. L., ALEKSUNES, L. M. & ZHU, H. 2020. Advancing computer-aided drug discovery (CADD) by big data and data-driven machine learning modeling. Drug discovery today.
32. ZHENG, W., BROOKS, B. R., DONIACH, S. & THIRUMALAI, D. 2005. Network of dynamically important residues in the open/closed transition in polymerases is strongly conserved. Structure, 13**,** 565-577.